Cognitive Radio Networking with Cooperative and Energy Harvesting

Ala'eddin Masadeh, Ahmed E. Kamal, Zhengdao Wang
Iowa State University (ISU), Ames, IA 50011, USA,
emails: {amasadeh,kamal,zhengdao}@iastate.edu

***Abstract*—Cognitive radio networks with energy harvesting result in efficient use of both energy and spectrum. By using cooperative relaying, another feature can be achieved, which is the high diversity gain. In this paper, an energy harvesting underlay cognitive radio relaying network is investigated. In this underlay cognitive radio scheme, secondary users are allowed to access the spectrum, respecting a certain primary interference threshold. The secondary nodes employ decode-and-forward relaying in order to maximize the total received data by optimizing their transmit powers. In this context, both the secondary source and relay harvest energy from renewable sources and store it in finite batteries. They are also capable of buffering data in infinite capacity buffers. We derive closed-form expressions for transmit power of secondary source and relay that maximize the secondary network throughput. Projected subgradient method is used to find the power allocated to the secondary network. Numerical simulations are conducted to study the performance of the proposed system. Comparisons are made between the proposed system and other conventional scenarios, and it is observed that when the required signal-to-interference-plus-noise ratio (SINR) at the primary receiver is high, the proposed harvesting-based scheme and conventional-based scheme perform similarly.**

***Index Terms*—Energy harvesting, underlay cognitive radio, cooperative relay.**

I. Introduction

Recently, energy harvesting has been considered as one of the promising solutions for sustainable wireless communications. Energy harvesting technology converts the ambient energy into usable electric energy [1]. Current energy harvesting techniques are able to provide limited levels of energy, e.g., an outdoor solar panel can get the benefit of 10 mW/cm^2 solar energy flux with harvesting efficiency taking values between 5% and 30%, depending on the used material [2]. At the same time, cooperative communication is one of the advanced technologies in wireless communications [3], [4], where the wireless nodes assist each other in delivering their data in order to achieve more reliable communication [5]. Combining energy harvesting with cooperative relaying can further achieve energy efficient reliable communication, in [6] the authors examined energy harvesting with cooperative communication system and energy transfer property. They assume that both source and relay can harvest energy from ambient environment. In addition, the relay can harvest energy radio frequency signals from the source. The framework objective is to maximize the end-to-end throughput by optimizing transmission powers and energy transfer. Moreover, cooperative communication can be used in cognitive radio networks in order to enhance the system performance, where the performance of the cognitive radio combined with cooperative relay outperforms the performance of the direct link communication (i.e., without relays) specially if the distance between the communication terminals is relatively large. Another important advantage of using relay system is that with such system, a diversity gain can be achieved [5].

Combining energy harvesting with cognitive radio aims to allocate the spectrum efficiently in a green manner [7]–[10]. In a cognitive radio underlay setup, both primary and secondary users access the spectrum simultaneously. In order to protect the primary Quality-of-Service (QoS), the interference from all secondary nodes should be kept under a certain tolerance limit [11]. For instance, the authors in [12] study the energy harvesting underlay cognitive radio network with cooperation between the secondary and the primary users, where the secondary user, who shares the spectrum owned by the primary, is equipped with energy harvesting capability and has finite capacity battery for energy storing. In return, the secondary user transfers portion of its energy to the primary user.

Integrating energy harvesting, cooperative communications, and cognitive radio was shown significant improvements [13], [14]. For instance, the authors in [13] studied a cooperative energy harvesting with cognitive overlay system, in which the secondary user utilizes portion of the primary time for its transmission data, in return, acting as a relay for the primary user, the secondary user can help in primary transmission. In their proposed model, two radio frequency energy harvesting techniques were used in the relay side. In [14], the authors investigated the problem of observing the secondary users sequentially to be used as cooperative relay to the primary transmitter. They derived an optimal stopping rule that selects a relay from a set of candidates to help in relay transmission, which maximizes the observation efficiency. However, to the best of the authors' knowledge, the underlay cognitive radio energy harvesting system assisted by buffered cooperative relaying nodes has not been considered in the literature.

In this work, underlay cognitive radio energy harvesting system assisted by a decode and forward relay is considered, where the secondary users can access the primary user frequency band by exploiting the allowance of its signal-to-interference-plus-noise ratio (SINR) constraints. Moreover, both the secondary source and relay are considered as buffer-aided nodes that can buffer infinite data and store finite energy. The main goal of this work is to derive the optimal power policy that maximizes the number of bits received by the secondary destination. Finally, the performance of the proposed scheme is analyzed to verify our findings, and compared with other schemes to check its validity and efficiency.

The remainder of the paper is organized as follows. Section II describes the proposed energy harvesting cognitive radio system. The problem formulation is given in Section III. Then, the proposed solution is discussed in Section IV. Numerical simulation results are presented in Section V. Finally, the paper is concluded in Section VI.

II. System Model

We consider a cooperative cognitive radio network with energy harvesting consisting of primary and secondary networks, as illustrated in Fig. 1. The primary network consists of primary source and destination nodes, denoted by PS and PD, respectively. The secondary network is a two-hop relay network consisting of a source, a relay, and a destination node denoted by SS, SR and SD, respectively. SS and SD are far away from each other, i.e., they are not in the coverage communication range of each other.

Each of the SS and SR is equipped with infinite data queue to buffer received data and finite battery to store harvested energy. It is assumed that there are always data packets in the data queue of the SS to be delivered to the SD, which causes depletion of the energy of the SS. Data packets are sent from SS to SR and then are transmitted from the SR to the SD, which causes depletion of the SR's energy. The SR is a full-duplex node, which can transmit and receive data at the same time. In this model, energy consumption is considered only due to data transmission, and it does not take into account any other energy consumption, such as processing, circuitry, etc.

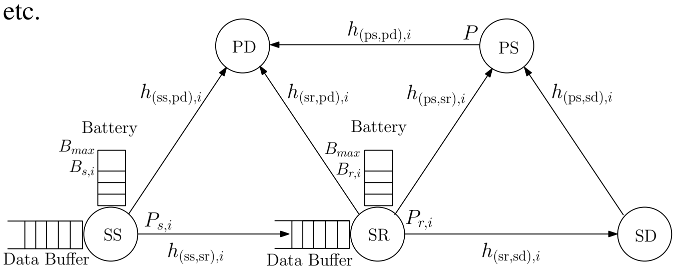

Fig. 1. Cooperative underlay cognitive radio system with energy harvesting.

We consider a time slotted system with M equal length time slots. In the secondary network, a decode and forward relaying protocol is used, where the SR can decode the SS signal before broadcasting it to the SD. It is assumed that updating the data queue and energy storage of the SR is delayed by one time slot with respect to the SS. Because of this delay, the efficiency of data transfer from the SS to SD is affected slightly. We assume that M is large so that the slight loss of inefficiency can be neglected.

Let the maximum capacity of the batteries is B_{max}. $B_{s,i}$ and $B_{r,i}$ represent the battery levels of both SS and SR, respectively, at time slot i. Each time slot is divided into two equal sub-slots for both transmitting and harvesting. Fig. 2 illustrates the slotted system model for both SS and SR. This model is designed such that the energy harvesting nodes first transmit their signals and then harvest energy, where the transmit power in the current slot depends only on the previous battery level. The batteries are assumed to be ideal, which means that there is no loss during retrieving or storing energy.

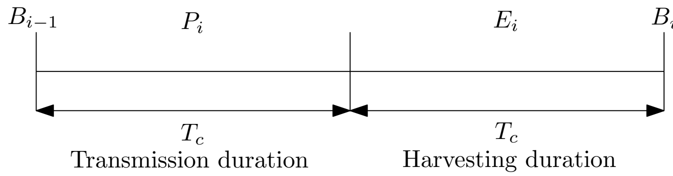

Fig. 2. Slotted system model.

The channels are Rayleigh fading channels. It is also assumed that we have full channel state information (CSI), and the channels are stationary within every time slot, i.e., $h_{(\text{a,b}),i}$ is constant during the ith time slot, where the channel between the nodes a and b at time slot i is given by

$$h_{(\text{a,b}),i} = \sqrt{d_{(\text{a,b})}^{\alpha_p}}\tilde{h}_{(\text{a,b}),i} \tag{1}$$

where $d_{(\text{a,b})}$ is the distance between the two nodes, α_p is a path loss constant, and $\tilde{h}_{(\text{a,b}),i}$ is the fading coefficient between a and b. Let us similarly define $h_{(\text{ss,sr}),i}$, $h_{(\text{sr,sd}),i}$, $h_{(\text{ss,pd}),i}$, $h_{(\text{sr,pd}),i}$, $h_{(\text{ps,pd}),i}$, $h_{(\text{ps,sd}),i}$ and $h_{(\text{ps,sr}),i}$ as the channel coefficients during the ith time slot between SS and SR, SR and SD, SS and PD, SR and PD, PS and PD, PS and SD, and PS and SR, respectively. The harvested energy at SS and SR during the ith time slot are denoted by $E_{s,i}$ and $E_{r,i}$, respectively. Two transmission cases are studied, case 1) SS keeps transmitting its data for all of the M slots, case 2) SS completes its transmission within T slots where $T < M$, after that, it keeps harvesting for $M - T$ slots without sending data to the SR. This gives the SR extra time $M - T$ to try sending all the data in its buffer. The latter case allows SR to receive data from the SS but not transmit them to the SD due to channel conditions, primary interference, or lack of harvested energy at the SR.

III. Problem Formulation

It is assumed that the PS transmits to the PD during all time slots. So, the received signal and the SINR at the PD side during the ith slot are, respectively, given as

$$y_i = \sqrt{P_i}h_{(\text{ps,pd}),i}x_i + n_{\text{pd},i}, \qquad i = 1, \ldots, M \tag{2}$$

$$\Gamma_i = \frac{P_i|h_{(\text{ps,pd}),i}|^2}{\sigma_n^2 + P_{s,i}|h_{(\text{ss,pd}),i}|^2 + P_{r,i}|h_{(\text{sr,pd}),i}|^2}, \qquad i = 1, \ldots, M \tag{3}$$

where P_i and x_i are the peak transmit power, and the transmitted signal by PS, respectively. $n_{\text{pd},i}$ is additive Gaussian noise with zero-mean and noise variance σ_n^2. The received signals at the SR and the SD during ith slot are, respectively, given as

$$y_{r,i} = \sqrt{P_{s,i}}h_{(\text{ss,sr}),i}x_{s,i} + n_{\text{sr},i}, \quad i = 1, \ldots, T \tag{4}$$

$$y_{d,i} = \sqrt{P_{r,i}}h_{(\text{sr,sd}),i}x_{r,i} + n_{\text{sd},i}, \quad i = 1, \ldots, M \tag{5}$$

where $P_{s,i}$ and $P_{r,i}$ are the peak power transmitted by SS and SR, respectively. $x_{s,i}$ and $x_{r,i}$ are the transmitted signals by SS and SR during the ith time slot, respectively. We assume that $n_{\text{sr},i}$ and $n_{\text{sd},i}$ are Gaussian, independent, zero mean, and they both also have variance σ_n^2. The SINR at the SR and SD are given, respectively, by

$$\Gamma_{r,i} = \frac{P_{s,i}|h_{(\text{ss,sr}),i}|^2}{\sigma_n^2 + P_i|h_{(\text{ps,sr}),i}|^2}, \quad i = 1, \dots, T \tag{6}$$

$$\Gamma_{d,i} = \frac{P_{r,i}|h_{(\text{sr,sd}),i}|^2}{\sigma_n^2 + P_i|h_{(\text{ps,sd}),i}|^2}, \quad i = 1, \dots, M \tag{7}$$

where the SR can remove the self interference by eliminating its own signal.

The objective is to optimize transmit powers for both SS and SR in order to maximize the sum rate between the SR and SD during M time slots, while satisfying the required QoS of the primary users, in addition to the data and energy causality constraints. The sum rate from SR to SD is given by

$$\max_{\{P_{s,i}, P_{r,i}, B_{s,i}, B_{r,i}\}} \sum_{i=1}^{M} \log(1 + \Gamma_{d,i}) \tag{8}$$

Thus, the energy causality constraints at SS and SR (i.e., the SS and SR cannot use more energy than their battery levels in the previous time slot), respectively, are given by

$$P_{s,i} T_c \le B_{s,i-1}, \quad i = 1, \dots, M \tag{9}$$

$$P_{r,i} T_c \le B_{r,i-1}, \quad i = 1, \dots, M \tag{10}$$

where T_c is the transmission duration. Since SS will keep silent (i.e. $P_{s,i} = 0$) after time slot T, the constraint in (9) can be written for all time slots.

Battery overflow constraints for both SS and SR (i.e., the update rules for the available energy in their batteries at the end of the current time slot, which are functions of the previous battery levels, in addition to transmit and harvested energy in the current time slot), respectively, are given by

$$B_{s,i} = \min\{B_{s,i-1} + E_{s,i} - P_{s,i} T_c, B_{max}\}, \quad i = 1, \dots, M \tag{11}$$

$$B_{r,i} = \min\{B_{r,i-1} + E_{r,i} - P_{r,i} T_c, B_{max}\}, \quad i = 1, \dots, M \tag{12}$$

Constraints (11) and (12) can be rewritten as follow

$$B_{s,i} \le B_{s,i-1} + E_{s,i} - P_{s,i} T_c, \qquad i = 1, \dots, M \tag{13}$$

$$B_{s,i} \le B_{max}, \qquad i = 1, \dots, M \tag{14}$$

$$B_{r,i} \le B_{r,i-1} + E_{r,i} - P_{r,i} T_c, \qquad i = 1, \dots, M \tag{15}$$

$$B_{r,i} \le B_{max}, \qquad i = 1, \dots, M \tag{16}$$

Without loss of generality, and for simplicity, it is assumed that T_c is normalized, hence, it is omitted from the following equations.

The following constraint is to ensure the data causality (i.e., the SR will not transmit the data to the SD before receiving it)

$$\sum_{k=1}^{i} \log(1 + \Gamma_{d,k}) \le \sum_{k=1}^{i} \log(1 + \Gamma_{r,k}), \quad i = 1, \dots, T \tag{17}$$

The data queue of the SR increases by $\log(1+\Gamma_{r,k})$ bit/Hz in the following time slot, when the SS transmits with $P_{s,i}$ to the SR during the ith slot. The same observation can be made at SD when the SR transmits with $P_{r,i}$. To grantee a QoS to the primary network, the following constraint should be satisfied

$$\Gamma_i \ge \gamma, \qquad i = 1, \dots, M \tag{18}$$

where γ is the predefined SINR QoS threshold at the PD. With simple manipulations, constraint (18) can be rewritten as

$$P_{s,i}|h_{(\text{ss,pd}),i}|^2 + P_{r,i}|h_{(\text{sr,pd}),i}|^2 \le I_{th,i}, \quad i = 1, \dots, M \tag{19}$$

where $I_{th,i}$ is given by

$$I_{th,i} = \frac{P_i|h_{(\text{ps,pd}),i}|^2}{\gamma} - \sigma_n^2, \quad i = 1, \dots, M \tag{20}$$

$P_{s,i}$, $P_{r,i}$, $B_{s,i}$ and $B_{r,i}$ should satisfy the following constraints

$$P_{s,i} \ge 0, \qquad i = 1, \dots, T \tag{21}$$

$$P_{s,i} = 0, \qquad i = T+1, \dots, M \tag{22}$$

$$P_{r,i} \ge 0, \qquad i = 1, \dots, M \tag{23}$$

$$B_{s,i}, B_{r,i} \ge 0, \qquad i = 1, \dots, M \tag{24}$$

Finally, the following constraint requires that the received data at SD during $M - T$ slots (during the time where the SS is not transmitting) is limited by the data in the SR buffer

$$\sum_{i=1}^{M} \log(1 + \Gamma_{d,i}) \le \sum_{i=1}^{T} \log(1 + \Gamma_{r,i}) \tag{25}$$

The end-to-end rate optimization problem that maximizes the sum rate between SR and SD can now be formulated as

$$\begin{aligned} &\max_{\{P_{s,i}, P_{r,i}, B_{s,i}, B_{r,i}\}} && \sum_{i=1}^{M} \log(1 + \Gamma_{d,i}) \\ &\text{subject to} && (9)\text{–}(10), (13)\text{–}(17), (19), (21)\text{–}(25) \end{aligned} \tag{26}$$

IV. Proposed Solution

The formulated optimization problem given in (26) is a non convex problem because of constraints (17) and (26). In the sequel, we will transform it to an equivalent convex form. Change of variables can be used as follows [6]. Let $C_{r,i} = \log(1 + \Gamma_{r,i})$, $C_{d,i} = \log(1 + \Gamma_{d,i})$.

For simplicity, let us define the following

$$\alpha_i = \frac{\sigma_n^2 + P_i|h_{(\text{ps,sr}),i}|^2}{|h_{(\text{ss,sr}),i}|^2}, \quad i = 1, \dots, T \tag{27}$$

$$\beta_i = \frac{\sigma_n^2 + P_i|h_{(\text{ps,sd}),i}|^2}{|h_{(\text{sr,sd}),i}|^2}, \quad i = 1, \dots, M \tag{28}$$

From (6), (7), (27), and (28), $P_{s,i}$ and $P_{r,i}$ can be written, respectively, as follows

$$P_{s,i} = \alpha_i \Gamma_{r,i} \tag{29}$$

$$P_{r,i} = \beta_i \Gamma_{d,i} \tag{30}$$

Therefore, the formulated optimization problem after transformation can be written as

$$
\begin{aligned}
&\max_{\{C_{d,i},C_{r,i},B_{s,i},B_{r,i}\}} \quad \sum_{i=1}^{M} C_{d,i} \\
&\sum_{k=1}^{i} C_{d,k} \le \sum_{k=1}^{i} C_{r,k}, && i=1,\dots,T \\
&\alpha_i(2^{C_{r,i}}-1) \le B_{s,i-1}, && i=1,\dots,M \\
&\beta_i(2^{C_{d,i}}-1) \le B_{r,i-1}, && i=1,\dots,M \\
&B_{s,i} \le B_{s,i-1}+E_{s,i}-\alpha_i(2^{C_{r,i}}-1), && i=1,\dots,M \\
&B_{s,i} \le B_{max}, && i=1,\dots,M \\
&B_{r,i} \le B_{r,i-1}+E_{r,i}-\beta_i(2^{C_{d,i}}-1), && i=1,\dots,M \\
&B_{r,i} \le B_{max}, && i=1,\dots,M \\
&\sum_{i=1}^{M} C_{d,i} \le \sum_{i=1}^{T} C_{r,i} \\
&\alpha_i(2^{C_{r,i}}-1)|h_{(\text{ss,pd}),i}|^2+\beta_i(2^{C_{d,i}}-1)|h_{(\text{sr,pd}),i}|^2 \\
&\qquad\qquad \le I_{th,i}, && i=1,\dots,M \\
&2^{C_{r,i}}-1 \ge 0, && i=1,\dots,T \\
&2^{C_{r,i}}-1 = 0, && i=T+1,\dots,M \\
&2^{C_{d,i}}-1 \ge 0, && i=1,\dots,M \\
&B_{s,i},B_{r,i} \ge 0, && i=1,\dots,M
\end{aligned} \tag{31}
$$

Now to transform the problem to a convex one, the last three constraints can be rewritten, respectively, as

$$-C_{r,i} \le 0, \quad i=1,\dots,T \tag{32}$$

$$C_{r,i} = 0, \quad i=T+1,\dots,M \tag{33}$$

$$-C_{d,i} \le 0, \quad i=1,\dots,M \tag{34}$$

Hence, the optimization problem becomes a convex problem, where the objective function is concave and the constraints are convex functions [15]. The Lagrangian of (31) is given in (35).

The Karush-Kuhn-Tucker (KKT) conditions are given as follows

$$-\sum_{i=k}^{T}\mu_i-\sigma_k-\xi+\alpha_k\ln(2)2^{C_{r,k}}\Big\{\theta_k+\eta_k + \psi_k|h_{(\text{ss,pd}),k}|^2\Big\}=0, \quad k=1,\dots,T \tag{36}$$

$$\nu_k+\alpha_k\ln(2)2^{C_{r,k}}\Big\{\theta_k+\eta_k+\psi_k|h_{(\text{ss,pd}),k}|^2\Big\}=0, \quad k=T+1,\dots,M \tag{37}$$

$$-1+\sum_{i=k}^{T}\mu_i-\rho_k+\xi+\beta_k(\ln(2))2^{C_{d,k}}\Big\{\omega_k+\lambda_k + \psi_k|h_{(\text{sr,pd}),k}|^2\Big\}=0, \quad k=1,\dots,T \tag{38}$$

$$-1-\rho_k+\xi+\beta_k(\ln(2))2^{C_{d,k}}\Big\{\omega_k+\lambda_k + \psi_k|h_{(\text{sr,pd}),k}|^2\Big\}=0, \quad k=T+1,\dots,M \tag{39}$$

Using (36) - (39), the closed form expressions can be obtained as

$$C^*_{r,k}=\begin{cases}(c_{r,1})^+, & k=1,\dots,T\\ (c_{r,2})^+, & k=T+1,\dots,M\end{cases} \tag{40}$$

$$C^*_{d,k}=\begin{cases}(c_{d,1})^+, & k=1,\dots,T\\ (c_{d,2})^+, & k=T+1,\dots,M\end{cases} \tag{41}$$

where

$$c_{r,1}=\log_2\left(\frac{\sum_{i=k}^{M}\mu_i+\sigma_k+\xi}{\alpha_k(\ln(2))\Big\{\theta_k+\eta_k+\psi_k|h_{(\text{ss,pd}),k}|^2\Big\}}\right) \tag{42}$$

$$c_{r,2}=\log_2\left(\frac{-\nu_k}{\alpha_k(\ln(2))\Big\{\theta_k+\eta_k+\psi_k|h_{(\text{ss,pd}),k}|^2\Big\}}\right) \tag{43}$$

$$c_{d,1}=\log_2\left(\frac{1-\sum_{i=k}^{M}\mu_i+\rho_k-\xi}{\beta_k(\ln(2))\Big\{\omega_k+\lambda_k+\psi_k|h_{(\text{sr,pd}),k}|^2\Big\}}\right) \tag{44}$$

$$c_{d,2}=\log_2\left(\frac{1-\sum_{i=k}^{M}\mu_i+\rho_k-\xi}{\beta_k(\ln(2))\Big\{\omega_k+\lambda_k+\psi_k|h_{(\text{sr,pd}),k}|^2\Big\}}\right) \tag{45}$$

and $(x)^+=\max(x,0)$. The closed form expressions for the optimal power levels can be obtained from (40), (41) and expressed as

$$P^*_{s,k}=\alpha_i(2^{C^*_{r,i}}-1) \tag{46}$$

$$P^*_{r,k}=\beta_i(2^{C^*_{d,i}}-1) \tag{47}$$

Note that the optimal powers are functions of the Lagrangian multipliers. To find the optimal Lagrangian multipliers, the projected subgradient method is employed [16]. In this method, any initial values of the Lagrangian multipliers can be used as a start points to evaluate the rates given in (40), (41). After that, projections of the primal variables on the constraints are computed, so that all values of $C_{r,k}$ and $C_{d,k}$ satisfy the feasibility of the solution, where the updated values of the optimal rates/powers and the Lagrangian multipliers are repeated until convergence. The Lagrangian multipliers at the next iteration $(n+1)$ are given as follows

$$\mu_k^{n+1}=\mu_k^n-\delta_{\mu,k}^n\Big[\sum_{i=1}^{k}(C_{d,i}-C_{r,i})\Big], \quad k=1,\dots,T \tag{48}$$

$$\theta_k^{n+1}=\theta_k^n-\delta_{\theta,k}^n\big[\alpha_k(2^{C_{r,k}}-1)-B_{s,k-1}\big], k=1,\dots,M \tag{49}$$

$$\omega_k^{n+1}=\omega_k^n-\delta_{\omega,k}^n\big[\beta_k(2^{C_{d,k}}-1)-B_{r,k-1}\big], k=1,\dots,M \tag{50}$$

$$\eta_k^{n+1}=\eta_k^n-\delta_{\eta,k}^n\big[B_{s,k}-B_{s,k-1}-E_{s,k}+\alpha_k(2^{C_{r,k}}-1)\big], \quad k=1,\dots,M \tag{51}$$

$$\lambda_k^{n+1}=\lambda_k^n-\delta_{\lambda,k}^n\big[B_{r,k}-B_{r,k-1}-E_{r,k}+\beta_k(2^{C_{d,k}}-1)\big], \quad k=1,\dots,M \tag{52}$$

$$\begin{aligned}\mathcal{L}=&-\sum_{i=1}^{M}C_{d,i}+\sum_{i=1}^{T}\mu_i\Big[\sum_{k=1}^{i}(C_{d,k}-C_{r,k})\Big]+\sum_{i=1}^{M}\theta_i\Big[\alpha_i(2^{C_{r,i}}-1)-B_{s,i-1}\Big]+\sum_{i=1}^{M}\omega_i\Big[\beta_i(2^{C_{d,i}}-1)-B_{r,i-1}\Big]\\&+\sum_{i=1}^{M}\eta_i\Big[B_{s,i}-B_{s,i-1}-E_{s,i}+\alpha_i(2^{C_{r,i}}-1)\Big]+\sum_{i=1}^{M}\lambda_i\Big[B_{r,i}-B_{r,i-1}-E_{r,i}+\beta_i(2^{C_{d,i}}-1)\Big]\\&+\sum_{i=1}^{M}\kappa_i\Big[B_{s,i}-B_{max}\Big]+\sum_{i=1}^{M}\phi_i\Big[B_{r,i}-B_{max}\Big]-\sum_{i=1}^{T}\sigma_iC_{r,i}+\sum_{i=T+1}^{M}\nu_iC_{r,i}+\xi\Big[\sum_{k=1}^{M}C_{d,k}-\sum_{k=1}^{T}C_{r,k}\Big]\\&+\sum_{i=1}^{M}\psi_i\Big[\alpha_i(2^{C_{r,i}}-1)|h_{(\mathrm{ss,pd}),i}|^2+\beta_i(2^{C_{d,i}}-1)|h_{(\mathrm{sr,pd}),i}|^2-I_{th,i}\Big]-\sum_{i=1}^{M}\rho_iC_{d,i}-\sum_{i=1}^{M}\varphi_iB_{s,i}-\sum_{i=1}^{M}\varrho_iB_{r,i}\end{aligned}\tag{35}$$

$$B_{s,k}^{n+1}=B_{s,k}^{n}-\delta_{s,k}^{n}\big[\eta_k-\eta_{k+1}-\theta_{k+1}+\kappa_k-\varphi_k\big],\quad k=1,\dots,M \tag{53}$$

$$B_{r,k}^{n+1}=B_{r,k}^{n}-\delta_{r,k}^{n}\big[\lambda_k-\lambda_{k+1}-\omega_{k+1}+\phi_k-\varrho_k\big],\quad k=1,\dots,M \tag{54}$$

$$\kappa_k^{n+1}=\kappa_k^{n}-\delta_{\kappa,k}^{n}\big[B_{s,k}-B_{max}\big],\quad k=1,\dots,M \tag{55}$$

$$\phi_k^{n+1}=\phi_k^{n}-\delta_{\phi,k}^{n}\big[B_{r,k}-B_{max}\big],\quad k=1,\dots,M \tag{56}$$

$$\sigma_k^{n+1}=\sigma_k^{n}-\delta_{\sigma,k}^{n}\big[-C_{r,k}\big],\quad k=1,\dots,T \tag{57}$$

$$\nu_k^{n+1}=\nu_k^{n}-\delta_{\nu,k}^{n}\big[C_{r,k}\big],\quad k=T+1,\dots,M \tag{58}$$

$$\rho_k^{n+1}=\rho_k^{n}-\delta_{\rho,k}^{n}\big[-C_{d,k}\big],\quad k=1,\dots,M \tag{59}$$

$$\psi_k^{n+1}=\psi_k^{n}-\delta_{\psi,k}^{n}\big[-I_{th,k}+\alpha_k(2^{C_{r,k}}-1)|h_{(\mathrm{ss,pd}),k}|^2+\beta_k(2^{C_{d,k}}-1)|h_{(\mathrm{sr,pd}),k}|^2\big],\quad k=1,\dots,M \tag{60}$$

$$\xi^{n+1}=\xi^{n}-\delta_{\xi}^{n}\Big[\sum_{i=1}^{M}C_{d,i}-\sum_{i=1}^{T}C_{r,i}\Big] \tag{61}$$

$$\varphi_k^{n+1}=\varphi_k^{n}-\delta_{\varphi,k}^{n}\big[-B_{s,k}\big],\quad k=1,\dots,M \tag{62}$$

$$\varrho_k^{n+1}=\varrho_k^{n}-\delta_{\varrho,k}^{n}\big[-B_{r,k}\big],\quad k=1,\dots,M \tag{63}$$

The step-sizes are updated according to the nonsummable diminishing step length policy [17]. We have also used constant step-size, which seems to work well also.

V. Simulation Results

In this section, simulation results are provided to demonstrate the performance of the proposed system model given in Fig. 1. In all simulation results, it is assumed that all the time slots are of length 1 second (i.e., $T_c = 1$ sec). The available bandwidth $B = 1$ MHz and the noise spectral density is $N_0 = 10^{-16}$ W/Hz, so that the noise variance $\sigma_n^2 = BN_0$. It is also considered that both of the SS and SR are equipped with solar panels of area of 100 cm^2 with 20% efficiency. Both SS and SR equipped with finite batteries of size $B_{max} = 5$ J. The initial battery levels of both SS and SR are zeros. The harvested energy levels are given by normal distribution with a mean equal to 0.2 and standard deviation equal to 0.033, where the harvested energy values are restricted to be between 0.1 and 0.3 Joule. Normal distribution is used as a distribution of the average harvested energy levels according to central limit theorem, where the sum of a large number of independent and identically distributed (i.i.d) variables is approximated by normal distribution [18]. The simulation is performed with $T = 5$ time slots and $M = 7$ time slots, unless otherwise stated. All channels are considered to be i.i.d Rayleigh fading channels, and the path loss exponent is equal to 4.

The distances between the communication nodes are assumed as $d_{(\mathrm{ss,sr})} = d_{(\mathrm{sr,sd})} = d_{(\mathrm{ps,pd})} = 50$ meters, corresponding to the distances between SS and SR, SR and SD, and PS and PD, respectively, and $d_{(\mathrm{ss,pd})} = d_{(\mathrm{sr,pd})} = d_{(\mathrm{ps,sd})} = d_{(\mathrm{ps,sr})} = 100$ meters, corresponding to the distances between SS and PD, SR and PD, PS and SD, and PS and SR, respectively.

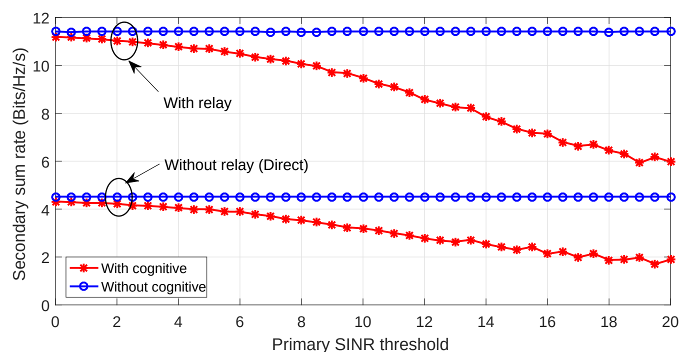

Fig. 3. Secondary sum rate of direct and relayed transmission systems with and without cognitive radio versus primary SINR.

Fig. 3 plots the maximum achievable secondary sum rate as a function of the pre-defined primary SINR threshold with and without cooperative relay. Thanks to relaying, it can be seen that using a relay increases the overall sum rate with considerable gap. This figure also shows that as the primary SINR threshold increases, the secondary sum rate decreases for both cases. This is due to the fact that by increasing the primary SINR threshold, the allowable transmit power of the secondary nodes should be reduced in order to respect this threshold. This figure also compares the proposed scheme without the interference constraint (i.e., no primary users in the system) as an upper bound (i.e., secondary nodes have flexibility to transmit with more powers). Fig. 4 compares the performance of the proposed system with two cases, when the secondary network uses energy harvesting technology, and when it uses non-harvested traditional batteries. One can see that, the performance of the traditional batteries outperforms the energy harvested with a considerable gap in the region where the primary SINR threshold is relatively small. However, this gap becomes smaller and smaller when the SINR

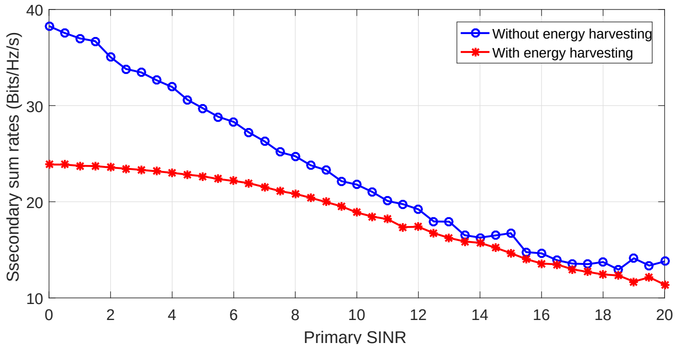

Fig. 4. Sum rate from the SR to the SD with and without energy harvesting versus different values for SINR at the primary network.

threshold is relatively large. This can be justified by the fact that with high values of SINR at the primary network, both models are restricted to transmit with low power to satisfy the primary QoS. In addition to the saving energy advantage, using energy harvesting technology becomes more interesting at the high values of the primary SINR threshold. Finally, Fig. 5

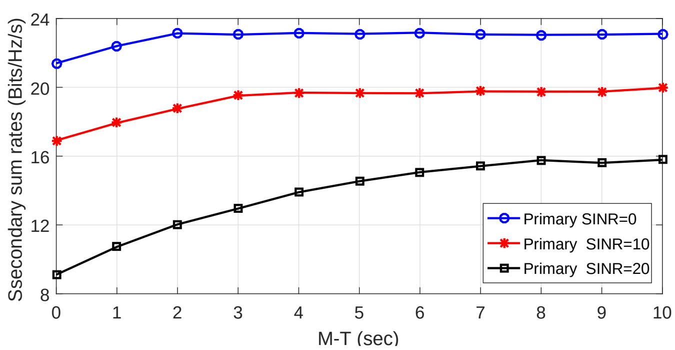

Fig. 5. The effect of increasing the extra time on sum rate the SR to the SD versus number of extra time slots.

shows the importance of having some extra slots $M-T$ that allow the relay to empty its data buffer. This can help the SD to avoid missing data that could not receive within the T time slots. This figure plots the sum rate between the SR and the SD versus the number of extra time slots $M-T$ for different values of primary SINR threshold. It can be shown that the sum rate can be increased up to a certain level, where adding more extra slots will not contribute to the rate, since the SR broadcast all the data in its buffer. The optimal number of $M-T$ time slots can be deduced from the figure for different values of the primary interference threshold $SINR = \{0, 10, 20\}$, where the optimal $M-T$ time slots increases as the SINR increases.

VI. Conclusions

In this paper, cooperative underlay cognitive radio network with energy harvesting was investigated, where the secondary users can access the primary frequency band by exploiting the allowance of the SINR constraint. Each of the secondary source and relay is equipped with infinite data buffer to carry data packets to be delivered and finite battery to store the harvested energy. We formulated an optimization problem aiming at maximizing the sum of the achievable rate over multiple time slots. After solving the problem using a projected subgradient method, the performance of the proposed scheme was investigated. Finally, we discussed the effect adding extra time for transmitting data from relay to destination that could not receive in allotted time. As a future work, the proposed model can be extended to solve the online optimization problem, where the harvested energy and the channels are unknown.

References

[1] M. Gregori and J. Gómez-Vilardebò, "Online learning algorithms for wireless energy harvesting nodes," in *Proc. of IEEE International Conference on Communications (ICC), Kuala Lumpur, Malaysia*, May 2016, pp. 1–6.

[2] R. Vullers, R. Schaijk, H. Visser, J. Penders, and C. Hoof, "Energy harvesting for autonomous wireless sensor networks," *IEEE Solid-State Circuits Magazine*, vol. 2, no. 2, pp. 29–38, Spring 2010.

[3] A. Sendonaris, E. Erkip, and B. Aazhang, "User cooperation diversity. part I. system description," *IEEE Transactions on Communications*, vol. 51, no. 11, pp. 1927–1938, Nov. 2003.

[4] J. N. Laneman, D. N. Tse, and G. W. Wornell, "Cooperative diversity in wireless networks: Efficient protocols and outage behavior," *IEEE Transactions on Information Theory*, vol. 50, no. 12, pp. 3062–3080, Dec. 2004.

[5] D. Hu and S. Mao, "Cooperative relay in cognitive radio networks: Decode-and-forward or amplify-and-forward?" in *Proc. of IEEE Global Telecommunications Conference (GLOBECOM), Miami, Florida, USA*, December 2010, pp. 1–5.

[6] B. Gurakan, O. Ozel, J. Yang, and S. Ulukus, "Energy cooperation in energy harvesting communications," *IEEE Transactions on Communications*, vol. 61, no. 12, pp. 4884–4898, Dec. 2013.

[7] X. Huang, T. Han, and N. Ansari, "On green-energy-powered cognitive radio networks," *IEEE Communications Surveys & Tutorials*, vol. 17, no. 2, 2015.

[8] X. Lu, P. Wang, D. Niyato, D. I. Kim, and Z. Han, "Wireless networks with RF energy harvesting: A contemporary survey," *IEEE Communications Surveys & Tutorials*, vol. 17, no. 2, 2015.

[9] R. Duan, M. Elmusrati, and R. Virrankoski, "Stable transmission for a cognitive-shared channel with rechargeable transmitters," in *Proc. of IEEE International Conference on Communications (ICC)*, Ottawa, Ontario, Canada, Jun. 2012, pp. 4632–4636.

[10] S. Park, H. Kim, and D. Hong, "Cognitive radio networks with energy harvesting," *IEEE Transactions on Wireless Communications*, vol. 12, no. 3, pp. 1386–1397, Mar. 2013.

[11] A. Alsharoa, H. Ghazzai, and M. S. Alouini, "Near-optimal power allocation with PSO algorithm for MIMO cognitive networks using multiple AF two-way relays," in *Proc. of IEEE International Conference on Communications (ICC), Sydney, Australia*, Jun. 2014, pp. 1580–1584.

[12] K. Pathak and A. Banerjee, "On energy cooperation in energy harvesting underlay cognitive radio network," in *Proc. of Twenty Second National Conference on Communication (NCC), Guwahati, India*, Mar. 2016, pp. 1–6.

[13] T. Kalluri and V. A. Bohara, "Regenerative relaying in energy harvesting cognitive radio networks," in *Proc. of European Conference on Networks and Communications (EuCNC), Athens, Greece*, Jun. 2016, pp. 84–88.

[14] T. Jing, S. Zhu, H. Li, X. Xing, X. Cheng, Y. Huo, R. Bie, and T. Znati, "Cooperative relay selection in cognitive radio networks," *IEEE Transactions on Vehicular Technology*, vol. 64, no. 5, pp. 1872–1881, May 2015.

[15] S. Boyd and L. Vandenberghe, *Convex optimization*. Cambridge university press, 2004.

[16] R. M. Freund, "Subgradient optimization, generalized programming, and nonconvex duality," *Massachusetts Institute of Technology*, 2004.

[17] S. Boyd and A. Mutapcic, "Subgradient methods," *Lecture notes of EE364b, Stanford University, Winter Quarter*, vol. 2007, 2006.

[18] D. Dehay, J. Leskow, and A. Napolitano, "Central limit theorem in the functional approach," *IEEE Transactions on Signal Processing*, vol. 61, no. 16, pp. 4025–4037, Aug. 2013.